Research Square

Preprints are preliminary reports that have not undergone peer review.
They should not be considered conclusive, used to inform clinical practice,
or referenced by the media as validated information.

The Effect of Sintering Temperature on Microstructure and Properties of 94wt% WC - 3wt% TiC - 6wt% Co Sintered by Spark Plasma Sintering

Vahid Aghaali (vahidaghaali@yahoo.com)
Iran University of Science and Technology https://orcid.org/0000-0002-7768-3845
Touradj Ebadzadeh
Materials and Energy Research Center
Seyed Mohammad Zahraee
Iranian Research Organization for Science and Technology
Seyed Mohammad Mirkazemi
Iran University of Science and Technology

Research Article

Keywords: Cemented carbide, spark plasma sintering (SPS), tungsten carbide(WC), titanium carbide(TiC), cobalt(Co)

Posted Date: August 24th, 2021

DOI: https://doi.org/10.21203/rs.3.rs-832398/v1

License: This work is licensed under a Creative Commons Attribution 4.0 International License.
Read Full License

Abstract

Cemented carbide 94wt% WC – 3wt% TiC – 6wt% Co was sintered by spark plasma sintering at various temperatures of 1200, 1300, and 1400°C and the effect of sintering temperature on the microstructure and properties of this type of hard metals, such as total density, apparent density, hardness, and fracture surface were measured and observed using Field Emission-Scanning Electron Microscopy(FE-SEM), Optical Microscopy (OM), X-ray diffractometry (XRD) and mechanical test instruments. The results showed that the apparent density of the samples increased with increasing sintering temperature from 1200℃ to1300℃ from 13.98 g/cm^3 to 14.23 g/cm^3, respectively. But in the case of sample sintered at 1400℃, the density was reduced to 14.20 g/cm^3. Also, micro-hardness results showed that the hardness of sintered samples increased with the increase of sintering temperature. For the sample sintered at 1200°C the hardness value of 1746.41HV was obtained which increased with increasing sintering temperature from 1300℃ to 1400℃ from 2094.33HV to 2280.97HV, respectively. At the optimum sintering temperature, it was found that TiC inhibited the grain growth of tungsten carbide and increased the hardness values. In addition, as expected, the grain growth of tungsten carbide increased with increasing sintering temperatures. Examination of the fracture surface of sintered samples at different temperatures also showed that brittle fracture involves fracture.

1. Introduction

Tungsten carbide-cobalt hard metals are among the materials that can endanger human health by causing allergies[1, 2]. However, these materials are still the most important compounds for industrial applications. These composites have many applications in various industries because of their high hardness (due to the presence of carbide phase), good fracture toughness, good abrasion resistance, and fracture resistance at high temperatures. Due to the presence of a metal phase in these materials, the mechanical properties and thermal shock behavior are improved. These hard metals are mainly used in the manufacture of tools, abrasive parts, cutting tools, and also as an important material in the manufacture of machinery and equipment[3, 4]. These materials include the high hardness of the hexagonal mono-tungsten carbide ceramic phase in which the space between tungsten carbide particles is filled by the soft phase of cobalt. With increasing amounts of tungsten mono-carbide in these materials, the hardness and wear resistance increase, while the fracture toughness decreases[4]. However, the mechanical properties of these materials may be reduced due to the de-carbonization of tungsten mono-carbide particles as well as the formation of secondary phases by penetration of carbon during the sintering process[5].

Achieving hard metals with higher hardness and fracture toughness is one of the most important demands of the industry. One way to improve the properties of these materials is to reduce the grain size of the primary powder. It has been reported that hardness and strength increase in structures with smaller grain sizes[3, 4]. It has also been shown that reducing the grain size of tungsten carbide below 500 nm has significantly improved the hardness, strength, and toughness of tungsten carbide-cobalt hard metals[6]. However, the rapid growth of very fine tungsten carbide particles occurs during the sintering of

these materials, even before the liquid phase is formed[7, 8]. Therefore, in order to improve the mechanical properties, it is necessary to prevent the growth of tungsten carbide particles during sintering. One of the best ways is to use tungsten carbide grain growth inhibitors[9, 10] such as Niobium carbide(NbC), Vanadium carbide(VC), Tantalum carbide(TaC), Hafnium carbide (HfC), Chromium carbide (Cr_2O_3), and Titanium carbide (TiC), etc[11]. One of the most important carbides used in Tungsten carbide-cobalt composites is Titanium carbide, which creates a solid solution during the sintering process and improves the properties of this type of composite. The dissolution of Titanium carbide particles in Tungsten carbide is low, even at high temperatures (around 2500°C), but the dissolution of Tungsten carbide particles in Titanium carbide is very high. Dependence of temperature on dissolution of tungsten carbide particles in titanium carbide and (W,Ti)C_{1-x} phase was reported by Metcalfe[12]. It has also been concluded that the dissolution of Titanium carbide particles in Tungsten carbide at 2500°C is the maximum value. The tungsten carbide particles, with 4.22 Angstrom lattice parameter, are immediately dissolved in titanium carbide with 4.32 Angstrom lattice parameter[12]. Ruddy et al[13]reported that at temperatures above 2530°C, there are titanium mono carbide and cubic phases with a melting point of approximately 3130°C with composition $(Ti_{0.54}W_{0.44})Co_{0.75}$.

It has been shown that traditional sintering methods in these materials increase the grain size of tungsten monocarbide, which causes a decrease in the desired properties. On the other hand, in many sintering methods, a very high sintering temperature is required to obtain full dense bodies[6, 14]. Many methods are used to sintering this type of material, including Hot pressing (HP)[15], Hot Isostatic Pressing (HIP) [16], microwave sintering [17], pulse plasma compaction (PPC) [18], and spark plasma sintering(SPS) [19], etc.

The use of the SPS technique due to the very high heating rate, as well as the very low maintenance time at sintering temperature and very low compression pressure variations, is one of the most important techniques. For these reasons, this technique is used to make nanocrystalline materials and cemented carbide (using fine-grain powders). The sintering mechanism in this method is based on the discharge of an electric spark in the material, which leads to a local increase in temperature up to 3000°C. Compared to other sintering methods, SPS is a method that due to special technology, has a very high rate of temperature increase and sintering time with this method is very short. For this reason, materials made with this method have an ideal microstructure as well as excellent mechanical properties[3, 14].

In the present work, 94wt% WC – 3wt% TiC – 6wt% Co hard material was sintered by the SPS method at three temperatures of 1200℃, 1300℃, and 1400℃, and the effect of sintering temperature on these hard materials was investigated.

2. Experimental Procedures

Tungsten carbide(WC), cobalt(Co) and titanium carbide(TiC) powders were used to make 94wt% WC – 3wt% TiC – 6wt% Co hard metals. Tungsten carbide powder and cobalt powder were prepared from Eurtungstene company with an average particle size smaller than 10 μm and titanium carbide powder

was prepared from Us-Nano Corporation with an average particle size between 40 and 60 nm and purity of more than 99% (> 99%) and cubic structure.

Then tungsten carbide, cobalt, and titanium carbide powders were weighed (for weighing the initial powders we used Sartorius type scales with a precision of 0/0001g). Then the mixing process was performed using planetary ball mills (Retsch PM400) with a ball-to-powder mass ratio of 4:1 and milling speed of 310 rpm by tungsten carbide-cobalt balls for 1 hour.

After mixing and homogenization, the powders were poured into graphite molds, and then the mold was placed in the SPS machine. In the next step, the necessary vacuum was set inside the chamber, then the process of making the bodies was performed at different sintering temperatures. The samples were sintered at three temperatures of 1200°C, 1300°C, and 1400°C with a sintering time of 10 minutes. For sintering the samples, the final pressure applied to the powder was 40 MPa and the electric current patterns were set as 12:2 (12 pulses on and 2 pulses off) and the heating rate was 50°C/min and the applied current intensity was also 1000 A.

The surfaces of the sintered samples were completely cleaned with a diamond grinding machine to remove the graphite layer and used for subsequent studies. After the grinding process, the surface preparation of samples was performed using sand blades P60, P280, P400, P800, P1000, P1200, and 2500, respectively. Then, samples were polished using diamond paste. After the polishing process, samples were etched in 37% hydrochloric acid solution and 30% hydrogen peroxide for 60 seconds.

The hardness of the samples was measured using the M5C-1000 machine made by Shab Sari Precision Equipment Company. To perform the hardness testing, an appropriate location was first detected using an existing microscope, and then a load of 1 kg was applied into the place within 20 seconds[20]. It should be noted that in each sample 5 points were considered and the final number was the average hardness number. To investigate the microstructure of the samples, the OLYMPUS BX60 Optical Microscope (Japan) and the Field Emission-SEM (Electron Scanning Electron Microscope) were used. Phase analysis of primary powders and sintered samples was performed using Bourevestnik DRON-8 ($Cu_{K-alpha1}$ =1.5406A). The phases in each sample were also analyzed using X'pert Highscore software.

The apparent density of sintered samples was determined using an Archimedes method. In this method, the density of samples was determined by comparing the weight in dry and immersed water. In this standard, the density of components was calculated as follows:

$$\rho_a = \frac{D}{D - I} \times \rho_L \qquad (1)$$

Also, the total density (mass or bulk) of the samples was obtained using the following formula:

$$\rho_b = \frac{D}{S - I} \times \rho_L \quad (2)$$

where

D: The sample weights in the air in a completely dry state

I: The weight of the sample in the fluid (water) in immersion

S: The weight of the saturation fraction of the liquid (water) in the air

ρ_b: Total density

ρ_a: Apparent density

ρ_L: Liquid density (water) at the desired temperature

To analyze the particle size and particle size distribution the images of Field Emission-SEM and Image J software were used. The dynamic light scattering method (PSA, Fritsch laser particle sizer analysette22) was also used to analyze the particle size and particle size distribution for the primary powders.

3. Results And Discussion

3.1. Evaluation of primary powders

Figure 1 shows the x-ray diffraction patterns for tungsten carbide, cobalt, and titanium carbide powders. As can be seen, the tungsten carbide powder used in this study has only mono-tungsten carbide (WC) peaks and peaks related to the W_2C phase are not seen in this powder which indicates the high purity of tungsten carbide powder (in terms of phase analysis). Also, in this powder, the peaks related to the mono-tungsten carbide phase have the maximum intensities at the angles of 2θ = 41.635 and 2θ = 56.728, which are related to plates (100) and (101), respectively. It can be seen that the peaks position and the intensity of peaks in titanium carbide powder are very similar to the standard sample (JCPDS/ICDD: 00-032-1383). The peak at 2θ = 48.839 has a maximum intensity, which is related to the (200) plates. The x-ray diffraction patterns of cobalt powder are shown in Fig. 1. As can be seen, the used cobalt powder has two types of allotropic. These two allotropic types of cobalt are close-packed hexagonal (ε) and face-centered cubic (α) which are shown in Fig. 1. It has been reported that the close-packed hexagonal type of cobalt (ε cobalt) is approximately stable at temperatures below 400°C and the face-centered cubic type of cobalt (α cobalt) is stable at higher temperatures[21]. It has also been reported that cobalt powders used in various industries contain approximately the same amounts of both types of allotropy. However, during the grinding or crushing process, the amount of hexagonal cobalt powder increases[22].

Scanning electron microscopy images of tungsten carbide, cobalt, and titanium carbide powders are shown in Fig. 2. As can be seen, tungsten carbide powder has a spherical shape with rounded and almost irregular corners. At higher magnifications, these quasi-spherical particles with rounded corners are more clearly seen (Fig. 2-A). Also, due to the presence of gravitational forces between the particles, agglomerates are observed in the primary powder. For cobalt powder, the particles also accumulate in the form of agglomerates in certain areas (Fig. 2-B). Electron microscopy images of titanium carbide powder are also shown in Fig. 2. As can be seen, the morphology of this powder is in the form of edged particles with sharp corners.

The results of particle size distribution analysis for tungsten carbide powder are shown in Fig. 3. It is observed that the particle size distribution for tungsten carbide powder is approximately 3 to 5 μm and most particles have a size of approximately 4 μm. It is also observed that 3.98% of the particles are smaller than 10 μm and 6.76% of the particles are smaller than 5 μm (d_{50} = 3.427μm).

3.2. Densification process and sintering phenomena

The variation of temperature and displacement (shrinkage) with time during the SPS process is shown in Fig. 4 (for samples sintered at 1200 ℃ and 1400 ℃ for 10 minutes). As can be seen, for the sintered sample at 1200 ℃ (Fig. 4-A), very little displacement (shrinkage) occurred approximately before 1500 seconds. This is due to the change in the grain arrangement and the filling of large cavities as well as the growth of tungsten carbide and titanium carbide particles (grain growth densification)[23]. Also, with a further increase in temperature, the displacement (contraction) increases (Approximately after 1500 seconds).

For the sintered sample at 1400 ℃ (Fig. 4-B), a slight displacement occurred approximately before 1700 seconds. But after this time, with increasing temperature, the displacement increases rapidly. Viscous flow densification and Liquid phase sintering, as well as particle rearrangement, are the most important factors in increasing the displacement at higher temperatures for these hard materials.

Furthermore, as shown in Fig. 4, the displacement for the sintered sample at 1400 ℃ is higher than for the sintered sample at 1200 ℃. This is due to the increased fluidity of the cobalt and the filling of porosity[24, 25].

It has been reported that during the heating process of powders, the volume decreases with increasing densification [23]. According to the SPS sintering mechanism, when the spark current flows through the powders, the temperature rapidly increases at the point of contact between the particles. As a result, according to the Joule Heating Effect, a temperature gradient is created from the center to the surfaces of the powder particles, and in a very small area, the temperature rises sharply. Cobalt melting also occurs at much lower temperatures, which leads to densification and filling of porosity [27].

3.3. Phase analysis (X-ray diffraction)

X-ray diffraction analysis for sintered samples at 1300 ℃ and 1400 ℃ is shown in Fig. 5. As can be seen, mono-tungsten carbide (WC) is the main phase in 94wt% WC – 3wt% TiC – 6wt% Co hard materials. The position of the low-intensity peaks of the cobalt (Co) and titanium carbide (TiC) phases is also shown in Fig. 5. It has been reported that the presence of titanium carbide particles in WC-TiC-Co hard materials creates a solid solution between tungsten carbide and titanium carbide[26, 27]. It has also been reported that increasing the sintering temperature can affect the solid solution phase amounts between tungsten carbide and titanium carbide[28] due to the increased diffusion process. It has been shown that the growth of this solid solution phase is controlled by the diffusion of atoms into the cobalt matrix[28]. As shown in Fig. 5, the solid solution peaks formed from the reaction between WC and TiC are not detectable due to the low amount of this phase. Low amounts of carbon in tungsten carbide-cobalt hard materials have been reported to lead to the formation of other phases (η phase). η phases include tungsten, cobalt, and carbon and these phases are unstable. For example, it has been reported that the $Co_{3.2}W_{2.8}C$ or Co_2W_4C phases may be converted to the cobalt, Co_6W_6C, and WC phases by a very slow reaction[29].

3.4. Microstructure, density, and mechanical properties

Figure 6 andFigure **7** show electron microscopy images of samples sintered at temperatures of 1200℃, 1300℃, and 1400℃. As can be seen, at a temperature of 1200℃ some tungsten carbide particles remain circular. As the sintering temperature increases to 1300℃, some circular particles are completely removed and angular particles with sharp edges of tungsten carbide are seen. It is also observed that by performing the sintering process at 1400℃, the particles also tend to grow abnormally. It has been reported that tungsten carbide particles grow and become larger in the sintering process by dissolution and deposition mechanism. Smaller particles dissolve in the binder phase and then begin to precipitate, and this phenomenon causes the smaller particles to disappear and the larger particles to grow[29]. At a temperature of 1200℃, very fine particles of tungsten carbide can be seen, but with increasing sintering temperature to 1400℃, the amount of these fine particles decreases, which is due to the dissolution of these particles in the cobalt matrix and finally the growth of tungsten carbide grains.

The particle size distribution analysis of tungsten carbide for sintered samples at different temperatures is also shown in Fig. 7.

As can be seen, the average particle size of tungsten carbide was obtained for sintered samples is 0.2, 0.3, and 0.7 μm for samples sintered at 1200, 1300, and 1400℃, respectively. Therefore, sintering temperature can affect the average particle size of tungsten carbide. In order to control the grain size of tungsten carbide, the addition of cubic carbides in this type of material has been proposed to improve some properties during the sintering process[30]. It is also very important to control the sintering temperature and determine the optimal sintering temperature.

It has been reported that there are many parameters to increase porosity in 94wt% WC – 3wt% TiC – 6wt% Co hard materials. Among the most important of these factors are the presence of impurities, lack of

homogeneity during mixing, trapped gases and sintering temperature. which prevents filling between the carbide particles by the binder phase[31].

In addition, as can be seen in these hard materials, tungsten carbide particles are dissolved in cobalt and the outer layers of the surfaces related to titanium carbide particles. The microstructure of these materials shows that parts of the tungsten carbide phase are replaced by the core-shell phase of TiC/(Ti, W)C. These observations have been reported in other studies[26, 28]. Figure 8 shows a schematic of the particles in these hard materials.

The density of sintered samples at different temperatures of 1200, 1300, and 1400°C is shown in Fig. 9. It can be seen that the apparent density of the samples increases with increasing sintering temperatures from 1200 to1300°C. This is due to increased cobalt phase fluidity and capillary pressure. Therefore, the porous is filled, and the amount of empty spaces between particles in the sample is reduced and the density is improved[11]. It has been reported that the wettability between tungsten carbide, titanium carbide and cobalt is highly dependent on the sintering temperature and wettability increases with increasing sintering temperature and sintering time. Increasing the atomic and liquid phase diffusion at the sintering temperature and decreasing the viscosity at high temperatures facilitate the movement of the liquid phase and leads to the filling of the pores and the improvement of the density[32]. As shown in Fig. 9, the apparent density decreases with increasing sintering temperature from 1300 to 1400°C. It has been reported that the density decreases with the excessive increase of sintering temperature by evaporation of Co[33]. Therefore, the use of the SPS method due to the short sintering time increases the density of samples compared to other sintering methods[34].

Figure 10 shows the increase of microhardness with the increase in sintering temperature from 1200 to 1400°C. For the sintered samples at 1200℃, 1300℃, and 1400℃, the microhardness values were 1746.41HV, 2094.34HV, and 2280.97HV, respectively. Therefore, the mechanical properties of 94wt% WC – 3wt% TiC – 6wt% Co hard materials depend on the size of tungsten carbide grains after the sintering process. Inhibiting the growth of tungsten carbide grains and reducing the grain size of tungsten carbide, increases the hardness of these materials[26]. Due to the higher amount of WC and higher its modulus of elasticity rather than cobalt and titanium carbide, when an external force is applied to these materials, a very large amount of this force is applied to the tungsten carbide grains. Therefore, the hardness of these materials depends on the grain size of tungsten carbide. It has been reported that when the cobalt amount in these materials is constant, there is a linear relationship between hardness and the grain size of tungsten carbide[35].

Although, titanium carbide has been reported to improve the hardness and abrasion resistance of these materials, but reduces the toughness[36]. Furthermore, creating a solid solution between titanium carbide particles and tungsten carbide and creating a core-shell structure including TiC-core/(W, Ti)C-shell can increase the hardness[26].

Two factors affect the growth mechanism of tungsten carbide grains with increasing sintering temperature. The first factor is the increase in cobalt phase fluidity with increasing sintering temperature.

Atomic mobility in the cobalt phase increases with increasing sintering temperature, which causes the pore in samples to fill faster. This factor increases the strength of the sample by increasing the density. The second factor is the increase in the diffusion coefficient of carbon and tungsten atoms in the cobalt phase with increasing sintering temperature. This factor also increases the growth rate of tungsten carbide grains. These two factors simultaneously affect the growth of tungsten carbide grains, and increasing the effect of one is associated with decreasing the effect of the other[11].

Electron microscopy images of the fracture surface of sintered samples at 1200, 1300, and 1400°C are shown in Fig. 11. As can be seen, the particle size increases with increasing sintering temperature from 1200 to 1400°C. Particles with abnormal size are also shown in Fig. 11-C. It is observed that with increasing sintering temperature to 1300°C, the porosity decreases. These results are consistent with the results for density(Fig. 9).

Investigating the fracture surface of the sintered samples at different temperatures indicates that the fracture mode in 94wt% WC – 3wt% TiC – 6wt% Co hard material is the brittle intergranular mode, and coarse WC fracture can be observed from the fracture surface. Since coarse WC grain can easily lead to stress concentration under loading conditions, so the micro crack generally originates from the rupture of coarse WC and the phase interface between coarse WC and binder. It is seen that the percentage of intergranular fracture is much higher than the percentage of transgranular fracture.

It is reported that the high intergranular fracture percentage in these materials is due to the high Young's modulus and the specific crystalline structure of tungsten carbide[37–39]. According to the Griffith-Orowan strength theory, the grain boundary strength between two tungsten carbide grains is 0.35 times the cleavage fracture strength of the tungsten carbide grain on the plate (100). And when a force is applied, the stress at the boundary between two tungsten carbide grains is greater than the stress at the tungsten carbide grain. This is the main reason for the higher percentage of intergranular fracture in this type of material[40].

It has been reported that very little plastic deformation occurs in these hard metals due to the fracture originating from micro-pores and coarse grains of tungsten carbide. The fracture of the sample occurs at the interface between the WC and Co phases and the crack grows through the Co phase. Therefore, the crack propagation is reduced by hard phases, and the fracture mode is observed as a brittle and intergranular fracture[40]. As can be seen in Fig. 11, the fracture morphology in these materials is relatively flat and the direction of cracks growth is relatively constant. Smooth plates caused by cleavage fracture create a lot of reflection. In all the specimens that were sintered at different temperatures, the fracture surfaces had a large reflection, and these surfaces were visible. Therefore, it can be concluded that fracture in cemented carbide with 6 wt% cobalt and 3 wt% of titanium carbide is a cleavage type.

Cleavage fracture is a brittle fracture that occurs along with certain crystallographic plates and is usually associated with small fracture energy. Cleavage sheets are the characteristics of any crystal lattice. Cleavage fracture has been observed in the structure of hcp, that tungsten carbide is one of the materials that has hcp structure[39].

4. Conclusions

In this research, the effect of sintering temperature on the microstructure and properties of 94wt% WC – 3wt% TiC – 6wt% Co hard materials were investigated. The most important results obtained are:

1) The microstructure of this type of cemented carbide depends on the sintering temperature and the grain size of tungsten carbide before and after the sintering process.

2) Performing the sintering process at low times and temperatures using the spark plasma sintering method and adding tungsten carbide grain growth inhibitors has a great effect on preventing abnormal growth of tungsten carbide grains.
3) For sintered samples at temperatures of 1200℃, 1300℃ and 1400℃, the average particle size of tungsten carbide was 0.2μm, 0.3μm, and 0.7μm, respectively. Therefore, increasing the sintering temperature increases the average particle size of tungsten carbide.
4) With increasing sintering temperature from 1200℃ to 1300℃, the density of the samples increased from 13.98 g/cm^3 to 14.23 g/cm^3, respectively. With a further increase in sintering temperature to 1400℃, the density was found to decrease to 14.20 g/cm^3.
5) The fracture mode of these materials is a brittle fracture. However, intergranular and transgranular fractures were observed at the fracture surface.

Declarations

Declaration of interests

 The authors declare that they have no known competing financial interests or personal relationships that could have appeared to influence the work reported in this paper.

 The authors declare the following financial interests/personal relationships which may be considered as potential competing interests:

References

1. Armstead AL, Li B (2016) "Nanotoxicity: emerging concerns regarding nanomaterial safety and occupational hard metal (WC-Co) nanoparticle exposure". Int J Nanomedicine 11:6421–6433
2. Lison D, Lauwerys R (1995) The interaction of cobalt metal with different carbides and other mineral particles on mouse peritoneal macrophages. Toxicol In Vitro 9:341–347 1995/06/01/
3. Liu W, Song X, Wang K, Zhang J, Zhang G, Liu X (2009) "A novel rapid route for synthesizing WC–Co bulk by in situ reactions in spark plasma sintering". Materials Science Engineering: A 499:476–481 2009/01/15/

4. Kim H-C, Shon I-J, Yoon J-K, Doh J-M, "Consolidation of ultra fine WC and WC–Co hard materials by pulsed current activated sintering and its mechanical properties," International Journal of Refractory Metals and Hard Materials, vol. 25, pp. 46–52, 2007/01/01/ 2007
5. Nino A, Takahashi K, Sugiyama S, Taimatsu H, "Effects of Carbon Addition on Microstructures and Mechanical Properties of Binderless Tungsten Carbide," MATERIALS TRANSACTIONS, vol. 53, pp. 1475–1480, 2012
6. Bao R, Yi J-h, Peng Y-d, Zhang H-z, Li A-k, "Decarburization and improvement of ultra fine straight WC–8Co sintered via microwave sintering," Transactions of Nonferrous Metals Society of China, vol. 22, pp. 853–857, 2012/04/01/ 2012
7. Mannesson K, Elfwing M, Kusoffsky A, Norgrent. S, Ågren. J, "Analysis of WC grain growth during sintering using electron backscatter diffraction and image analysis." International Journal of Refractory Metals & Hard Materials, pp. 449–455, 2008
8. Upadhyaya GS, "5 - Sintering Behavior of Cemented Carbides" in Carbides CT, Upadhyaya GS, Eds., (ed) Westwood: William Andrew Publishing, 1998, pp 138–165
9. Xiao D-h, He Y-h, Luo W-h, Song M, "Effect of VC and NbC additions on microstructure and properties of ultrafine WC-10Co cemented carbides," Transactions of Nonferrous Metals Society of China, vol. 19, pp. 1520–1525, 2009/12/01/ 2009
10. Wang H, Webb T, Bitler JW (2015) "Different effects of Cr3C2 and VC on the sintering behavior of WC–Co materials". International Journal of Refractory Metals Hard Materials 53:117–122 2015/11/01/
11. Mahmoodan M, Aliakbarzadeh H, Gholamipour R (2011) Sintering of WC-10%Co nano powders containing TaC and VC grain growth inhibitors. Transactions of Nonferrous Metals Society of China 21:1080–1084 2011/05/01/
12. Metcalfe AG, "The Mutual Solid Solubility of Tungsten Carbide and Titanium Carbide" Journal of the Institute of Metals, vol. 73, p. 591, 1946–47
13. Upadhyaya GS, "2 - Crystal Structure and Phase Equilibria" in Carbides CT, Upadhyaya GS, Eds., (ed) Westwood: William Andrew Publishing, 1998, pp 7–54
14. Deorsola FA, Vallauri D, Ortigoza Villalba GA, Benedetti BD, "Densification of ultrafine WC–12Co cermets by Pressure Assisted Fast Electric Sintering," International Journal of Refractory Metals and Hard Materials, vol. 28, pp. 254–259, 2010/03/01/ 2010
15. Jia C, Sun L, Tang H, Qu X, "Hot pressing of nanometer WC–Co powder," International Journal of Refractory Metals and Hard Materials, vol. 25, pp. 53–56, 2007/01/01/ 2007
16. Wei C, Song X, Zhao S, Zhang L, Liu W (2010) In-situ synthesis of WC–Co composite powder and densification by sinter-HIP. International Journal of Refractory Metals Hard Materials 28:567–571 2010/09/01/
17. Bao R, Yi J (2013) Effect of sintering atmosphere on microwave prepared WC–8wt.%Co cemented carbide. International Journal of Refractory Metals Hard Materials 41:315–321 2013/11/01/

18. Raihanuzzaman RM, Rosinski M, Xie Z, Ghomashchi R, "Microstructure and mechanical properties and of pulse plasma compacted WC - Co" International Journal of Refractory Metals and Hard Materials, vol. 60, pp. 58–67, 2016/11/01/ 2016
19. Rumman MR, Xie Z, Hong S-J, Ghomashchi R (2015) Effect of spark plasma sintering pressure on mechanical properties of WC–7.5wt% Nano Co. Materials Design 68:221–227 2015/03/05/
20. Kumar D, Singh K, "High hardness-high toughness WC-20Co nanocomposites: Effect of VC variation and sintering temperature" Materials Science and Engineering: A, vol. 663, pp. 21–28, 2016/04/29/ 2016
21. Betteridge W, Cobalt and Its Alloys: E. Horwood (January 1, 1982), 1982
22. Tikkanen MH, Taskinen A, Taskinen P, "Characteristic properties of cobalt powder suitable for hard metal production," Powder Metallurgy, vol. 18, p. 259, 1975
23. Oliver CJRG, Álvarez EA, García JL, "Kinetics of densification and grain growth in ultrafine WC-Co composites" International Journal of Refractory Metals and Hard Materials, vol. 59, pp. 121–131, 2016/09/01/ 2016
24. Liu K, Wang Z, Yin Z, Cao L, Yuan J, "Effect of Co content on microstructure and mechanical properties of ultrafine grained WC-Co cemented carbide sintered by spark plasma sintering," Ceramics International, vol. 44, pp. 18711–18718, 2018/10/15/ 2018
25. García J, Collado Ciprés V, Blomqvist A, Kaplan B (2019) Cemented carbide microstructures: a review. International Journal of Refractory Metals Hard Materials 80:40–68 2019/04/01/
26. Lee KH, Cha SI, Kim BK, Hong SH, "Effect of WC/TiC grain size ratio on microstructure and mechanical properties of WC–TiC–Co cemented carbides," International Journal of Refractory Metals and Hard Materials, vol. 24, pp. 109–114, 2006/01/01/ 2006
27. Szutkowska M, Boniecki M, Cygan S, Kalinka A, Grilli ML, Balos S, "Fracture behaviour of WC-Co hardmetals with WC partially substituted by titanium carbide" vol. 329, 2018
28. Yoon B-K, Lee B-A, Kang S-JL, "Growth behavior of rounded (Ti,W)C and faceted WC grains in a Co matrix during liquid phase sintering," Acta Materialia, vol. 53, pp. 4677–4685, 2005/10/01/ 2005
29. Upadhyaya GS, "6 - Microstructural Aspects of Cemented Carbides" in Carbides CT, Upadhyaya GS, Eds., (ed) Westwood: William Andrew Publishing, 1998, pp 166–192
30. Kaçmaz D, Kalkavan F, Yazıcı S, a. DA (2019) B. T., "Processing, Sintering and Performance of WC-Co-Near-Nano TiC Metal Matrix Composites.". Department of Mechanical Engineering, Dogus University, Turkey
31. Upadhyaya GS, "4 - Consolidation of Cemented Carbides" in Carbides CT, Upadhyaya GS, Eds., (ed) Westwood: William Andrew Publishing, 1998, pp 89–137
32. Jialin Sun J, Zhao Z, Li X, Ni Y, Zhou, Li A, "Effects of initial particle size distribution and sintering parameters on microstructure and mechanical properties of functionally graded WC-TiC-VC- Cr3C2-Co hard alloys.," 2016

33. Qiumin, Yang, JiangaoYang, HailinYang, and JianmingRuan "The effects of fine WC contents and temperature on the microstructure and mechanical properties of inhomogeneous WC-(fine WC-Co) cementedcarbides," 2016
34. Cha SI, Hong SH, Kim BK (2003) Spark plasma sintering behavior of nanocrystalline WC–10Co cemented carbide powders. Materials Science Engineering: A 351:31–38 2003/06/25/
35. H.F.Fischmeister, "Development and present status of the science and technology of hard materials," presented at the Proceedings of 1st International Conference on Science of Hard Materials, USA, New York: Plenum Press, 1983
36. Szutkowska M, Boniecki M, Cygan S, Kalinka A, Grilli M, Balos S, Fracture behaviour of WC-Co hardmetals with WC partially substituted by titanium carbide vol. 329, 2018
37. Hibbs MK, Sinclair R, Rowcliffe DJ (1984) "Defect interactions in deformed WC" Acta Metallurgica 32:941–947 1984/06/01/
38. Hibbs MK, Sinclair R (1981) Room-temperature deformation mechanisms and the defect structure of tungsten carbide. Acta Metall 29:1645–1654 1981/09/01/
39. Zhou W, Xiong J, Wan W, Guo Z, Lin Z, Huang S et al., "The effect of NbC on mechanical properties and fracture behavior of WC–10Co cemented carbides," International Journal of Refractory Metals and Hard Materials, vol. 50, pp. 72–78, 2015/05/01/ 2015
40. Sun L, Yang Te, Jia C, Xiong J (2011) "VC, Cr3C2 doped ultrafine WC–Co cemented carbides prepared by spark plasma sintering". International Journal of Refractory Metals Hard Materials 29:147–152 2011/03/01/

Figures

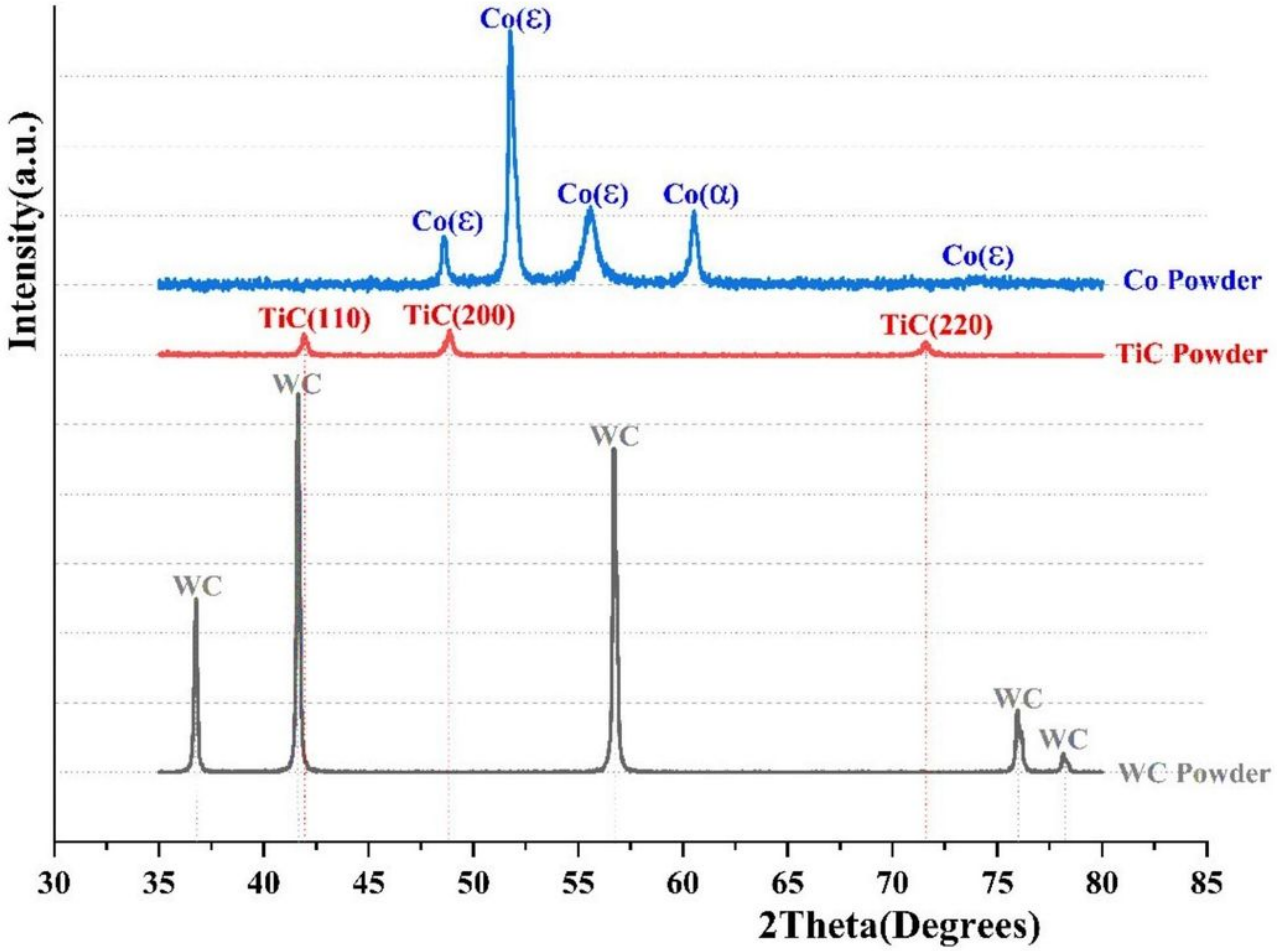

Figure 1

X-ray diffraction patterns for tungsten carbide(WC), cobalt(Co) and titanium carbide (TiC) powder.

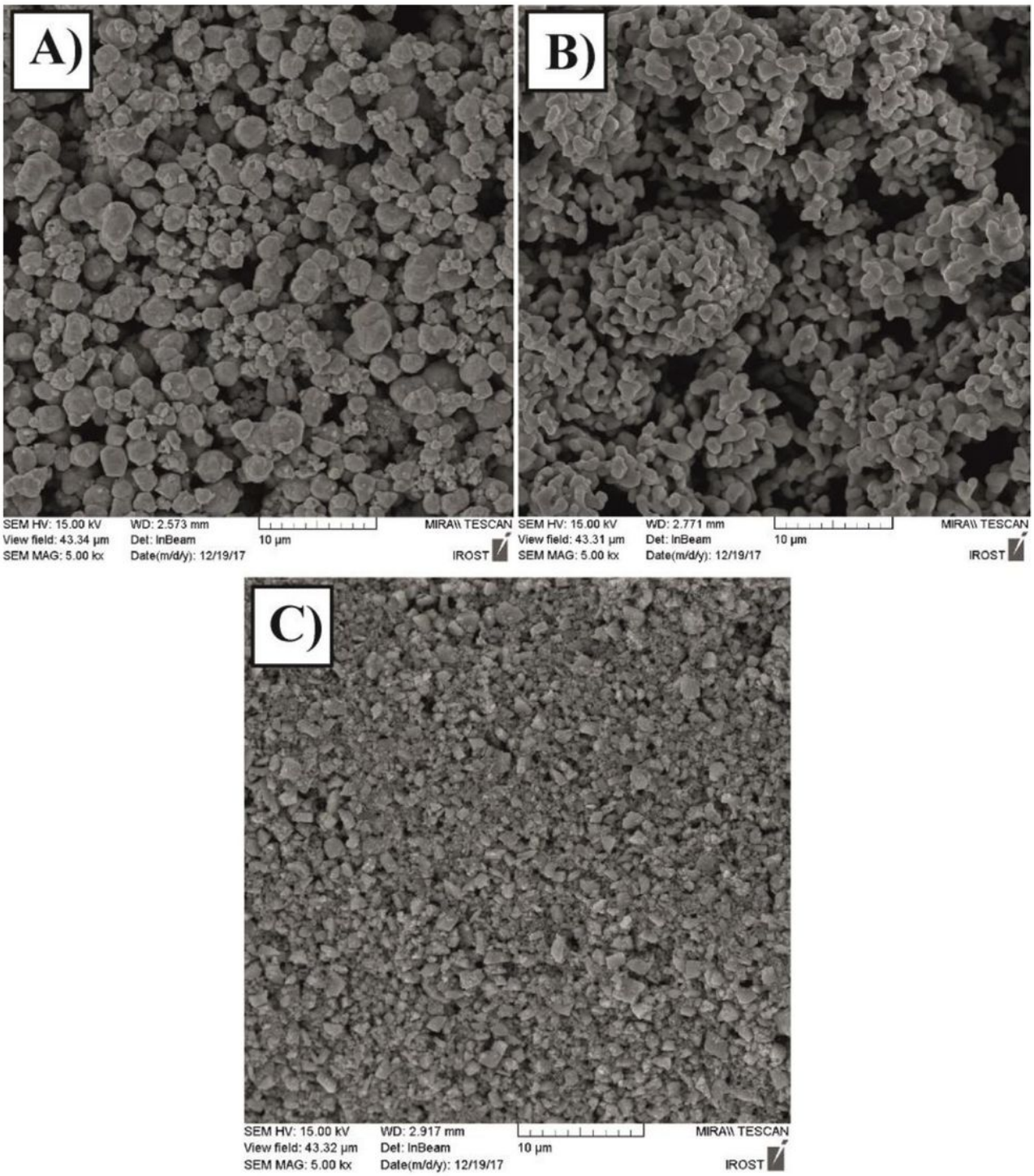

Figure 2

Scanning electron microscopy images of A) tungsten carbide powder B) cobalt powder and C) titanium carbide powder.

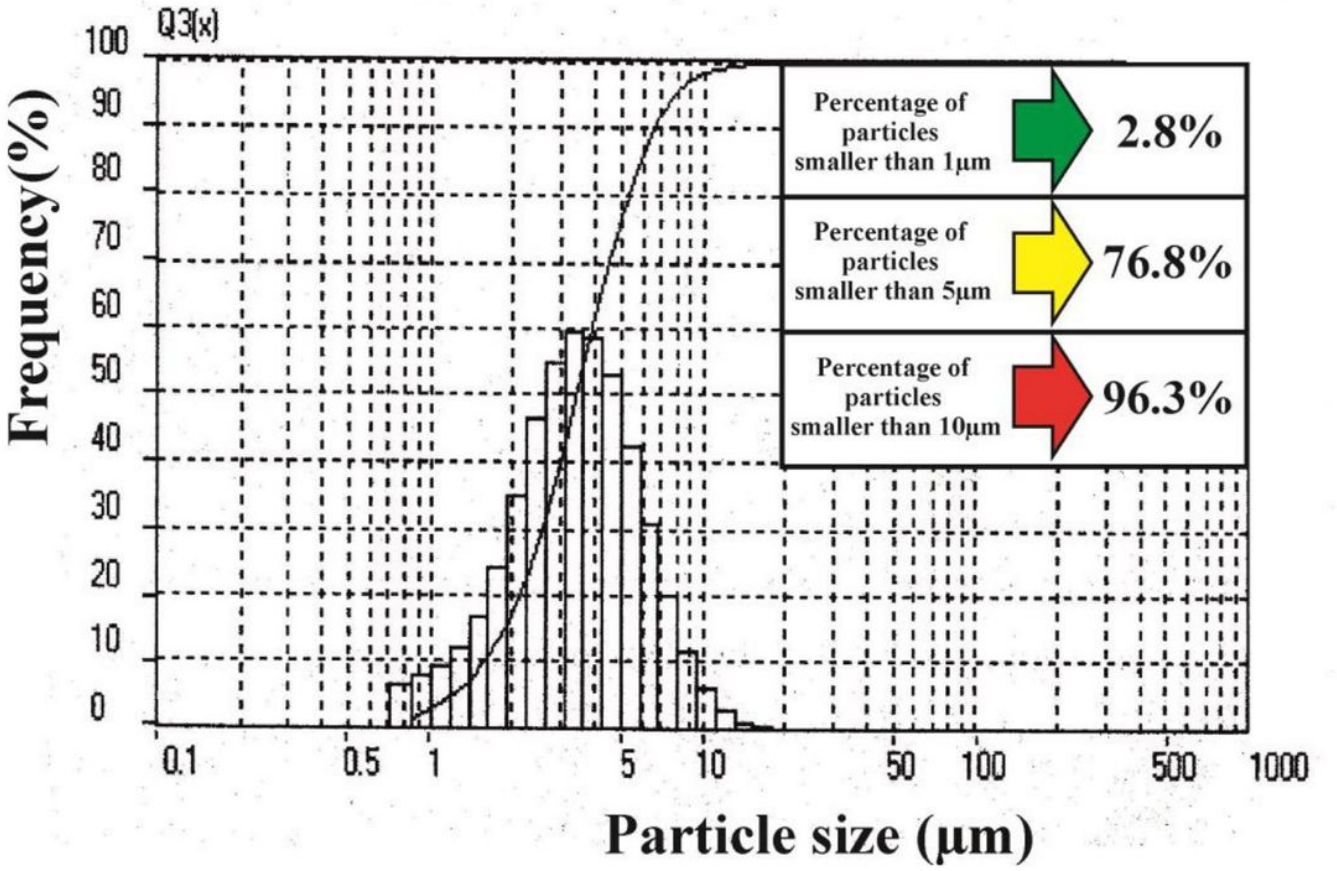

Figure 3

Particle size distribution analysis of tungsten carbide powder.

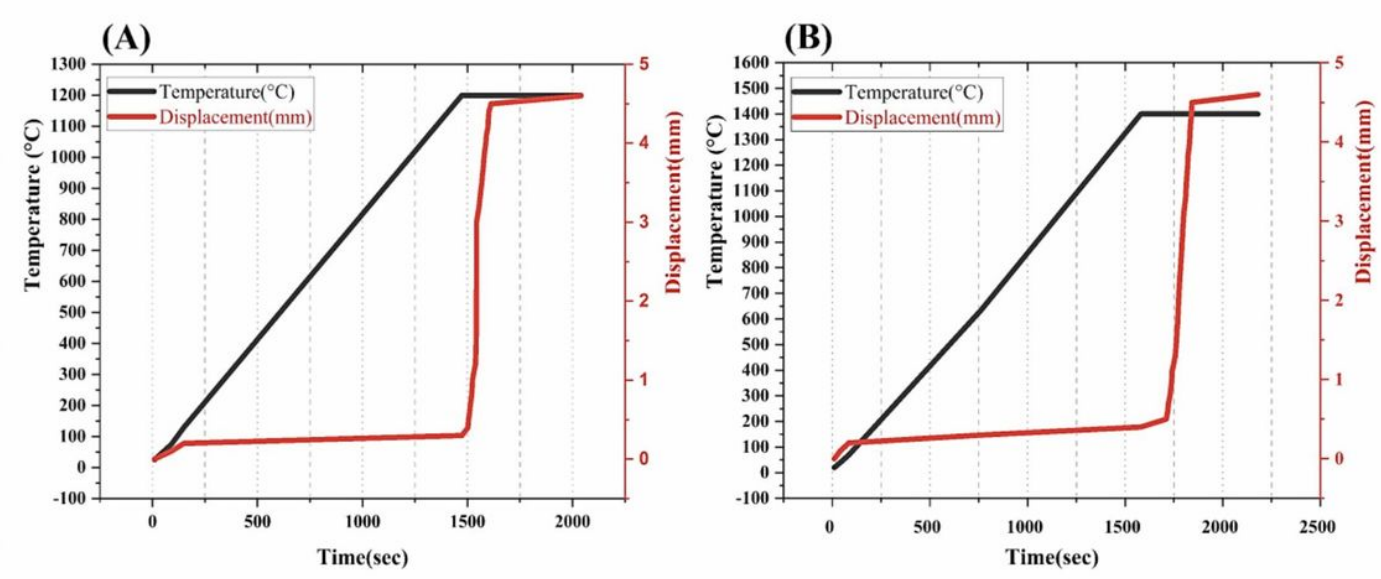

Figure 4

The variation of temperature and displacement with the time during the SPS process A) 1200°C and B) 1400°C.

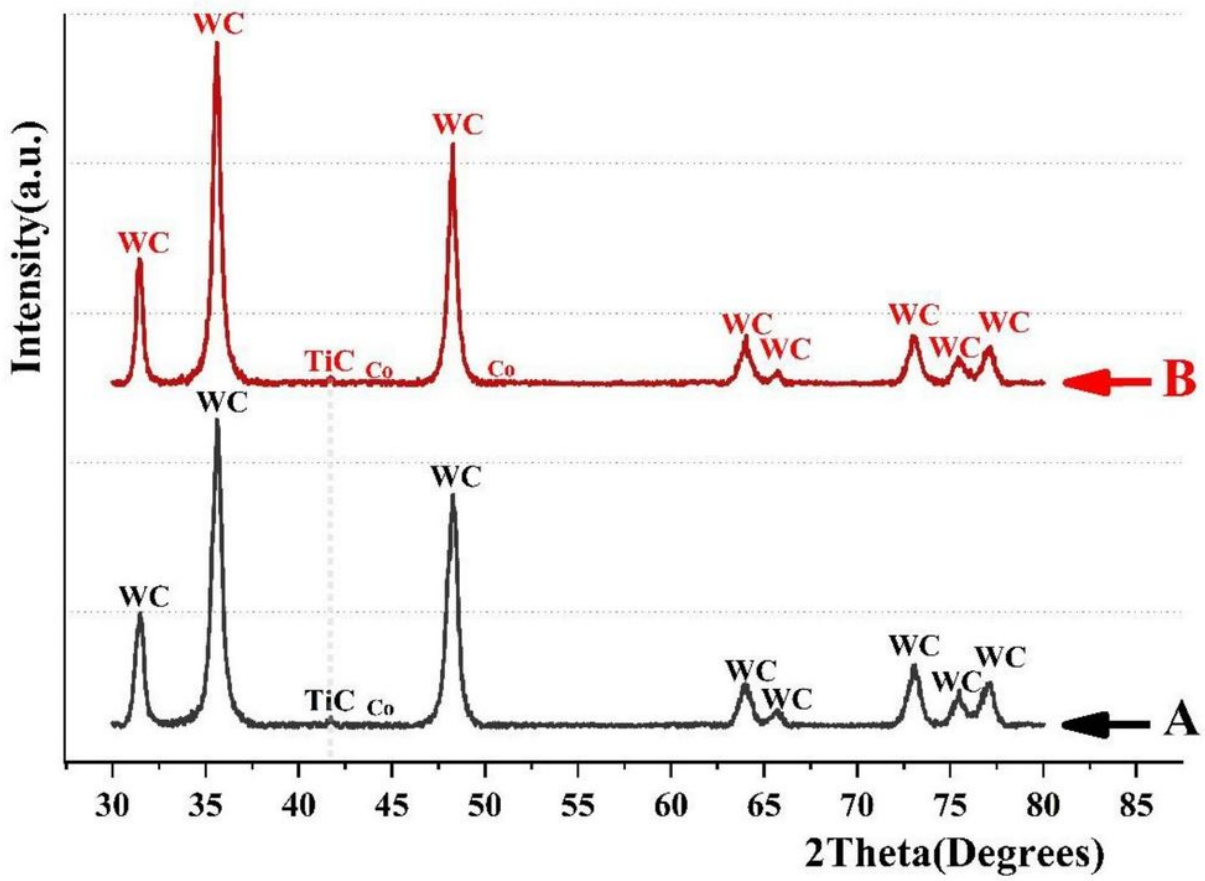

Figure 5

X-ray diffraction analysis for sintered samples at different temperatures A) 1300 °C and B) 1400 °C.

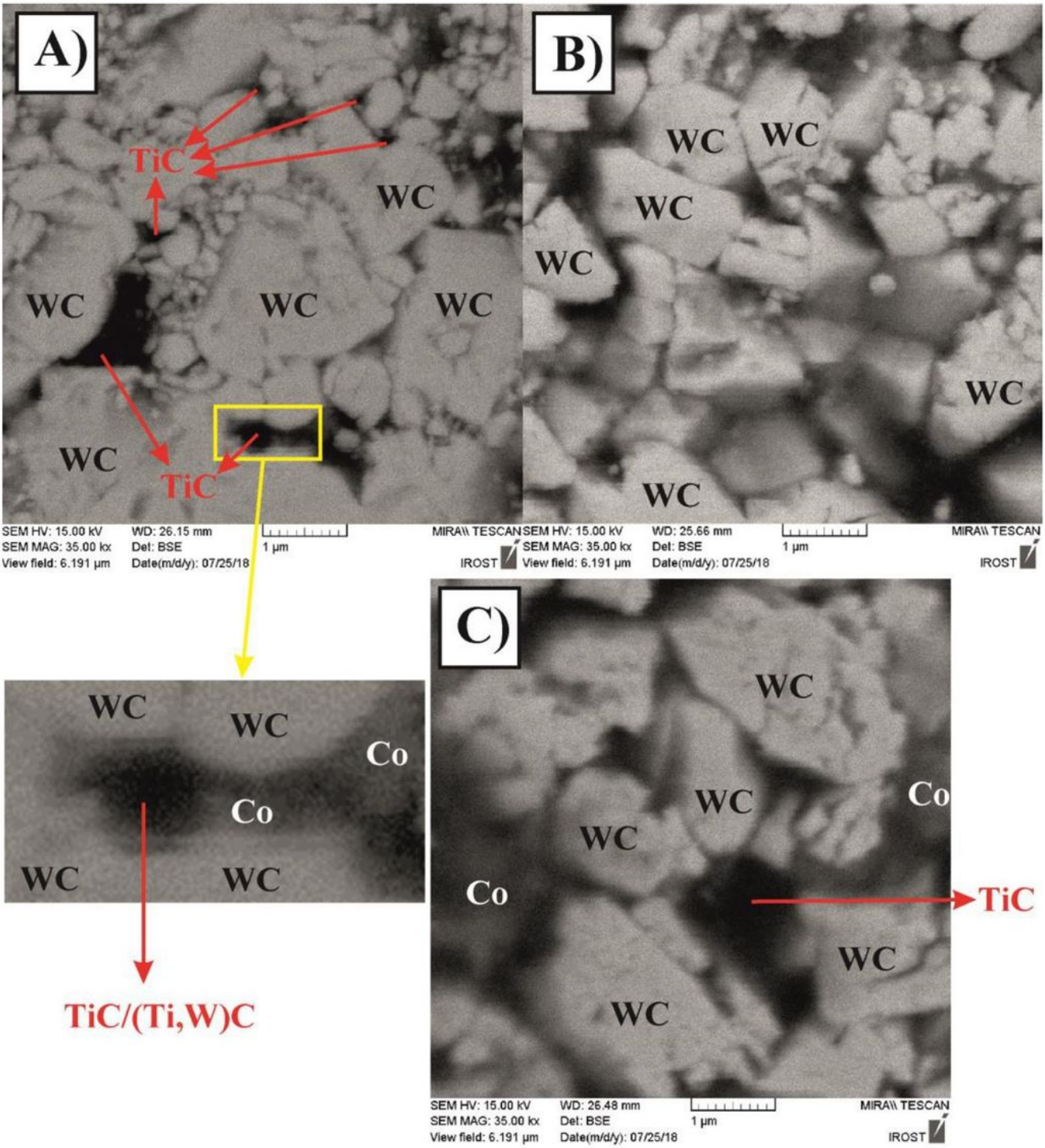

Figure 6

Electron microscopy images of samples sintered at different temperatures A) 1200 °C B) 1300 °C and C) 1400 °C.

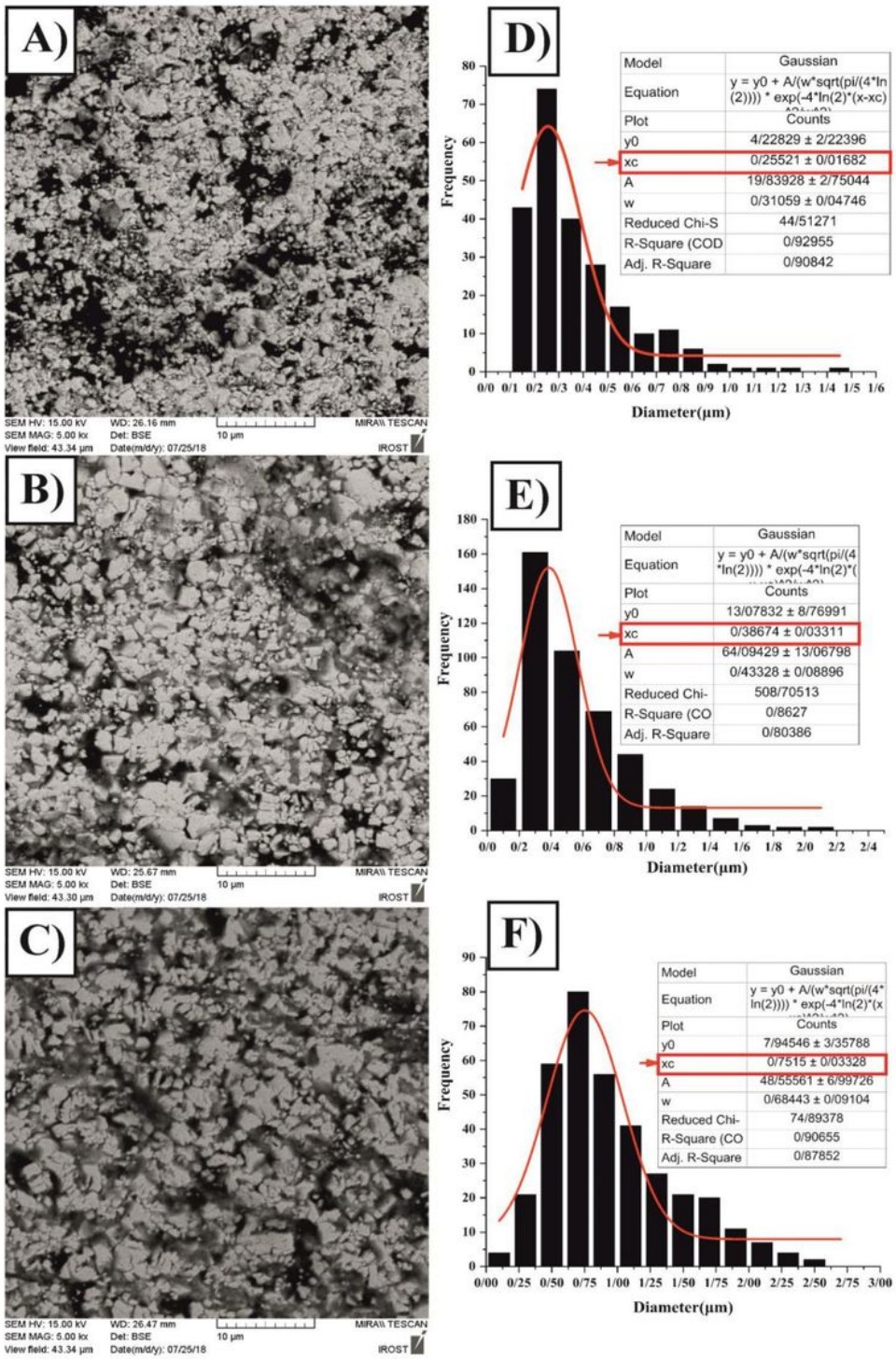

Figure 7

Electron microscopy images and particle size analysis of samples sintered at different temperatures A, D) 1200 °C and B, E) 1300 °C and C, F) 1400 °C.

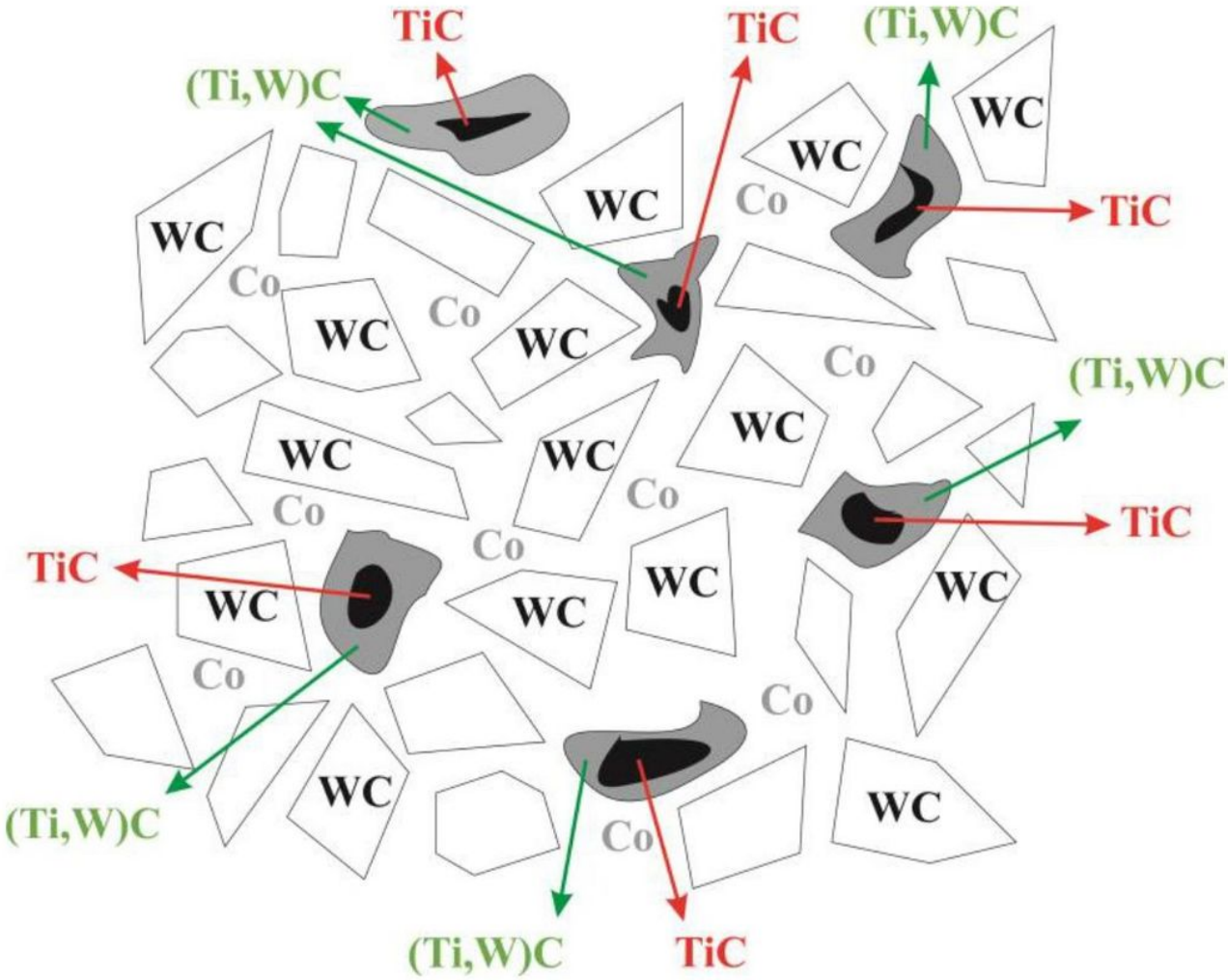

Figure 8

Schematic of hard metals 94wt% WC - 3wt% TiC - 6wt% Co.

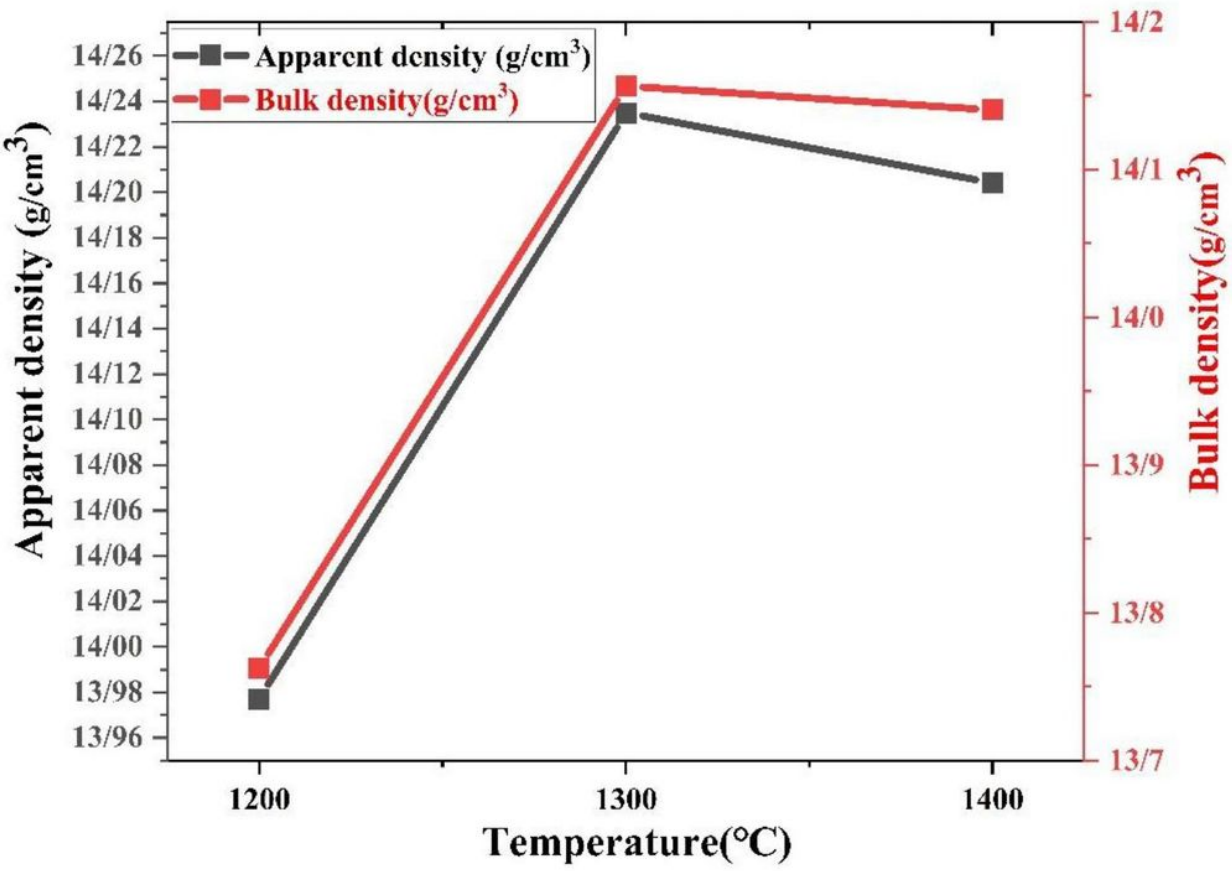

Figure 9

Apparent density and total density for sintered samples at different temperatures of 1200, 1300, and 1400 °C.

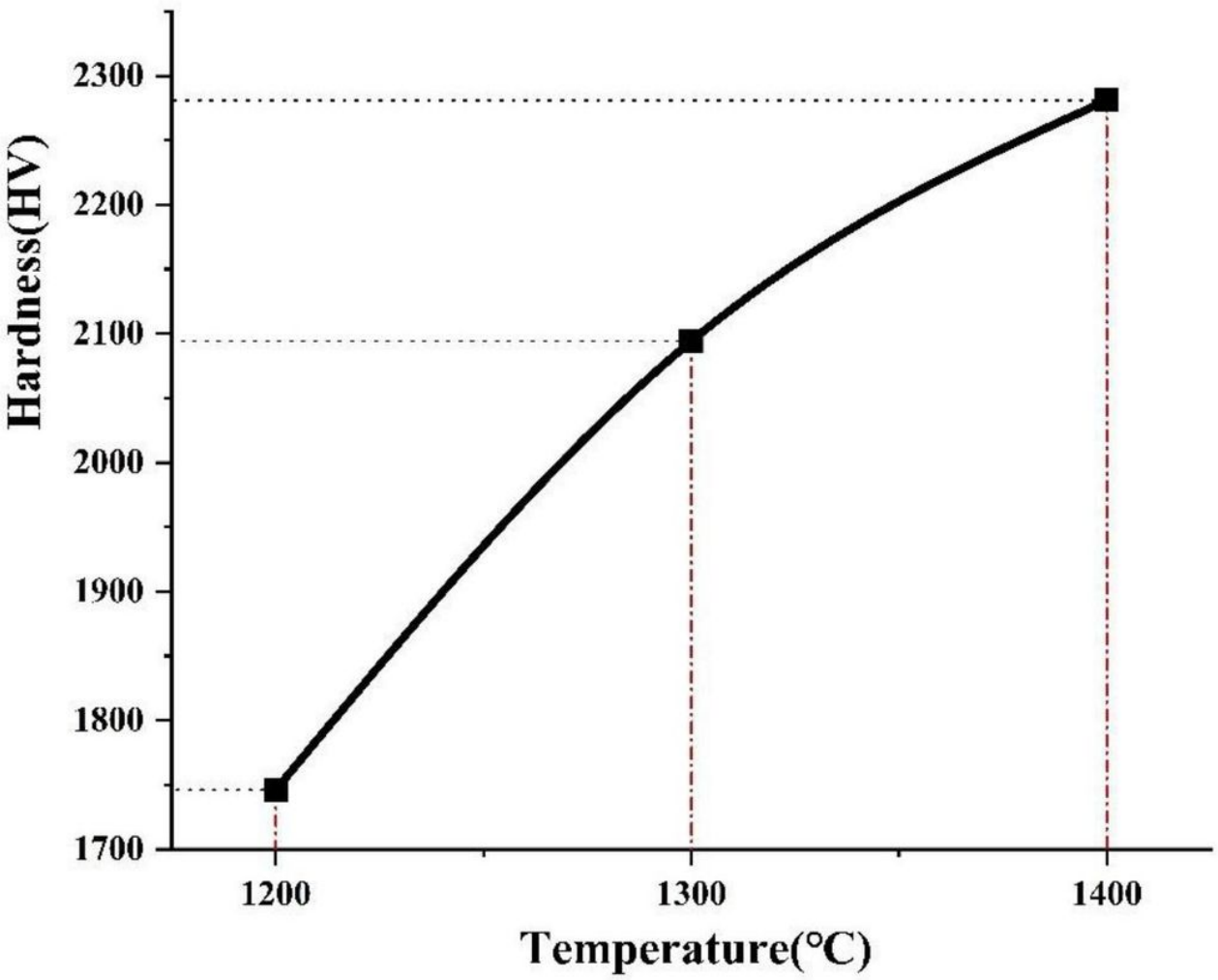

Figure 10

Microhardness results of sintered samples at different temperatures of 1200, 1300, and 1400 °C.

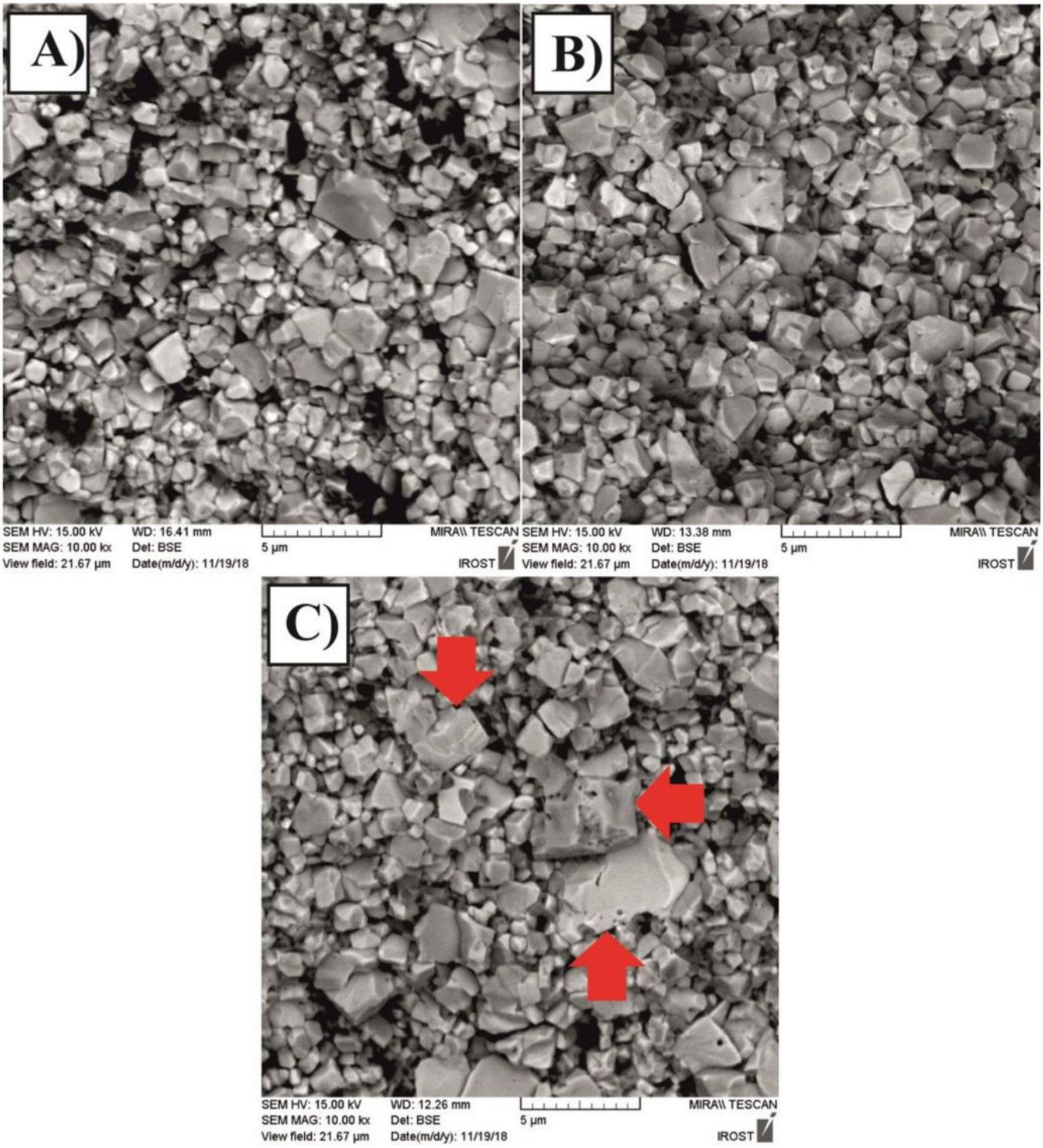

Figure 11

Electron microscopy images of the fracture surface of sintered samples at different temperatures A) 1200°C, B) 1300°C and C) 1400°C.